

Provided for non-commercial research and education use.
Not for reproduction, distribution or commercial use.



This article was published in an Elsevier journal. The attached copy is furnished to the author for non-commercial research and education use, including for instruction at the author's institution, sharing with colleagues and providing to institution administration.

Other uses, including reproduction and distribution, or selling or licensing copies, or posting to personal, institutional or third party websites are prohibited.

In most cases authors are permitted to post their version of the article (e.g. in Word or Tex form) to their personal website or institutional repository. Authors requiring further information regarding Elsevier's archiving and manuscript policies are encouraged to visit:

<http://www.elsevier.com/copyright>



ELSEVIER

Available online at www.sciencedirect.com

Theoretical and Applied Fracture Mechanics 48 (2007) 127–139

**theoretical and
applied fracture
mechanics**

www.elsevier.com/locate/tafmec

Softening behaviour and correction of the fracture energy

T.A.C.M. van der Put *

*TU Delft, Faculty of Civil Engineering and Geosciences, Timber Structures and Wood Technology,
P.O. Box 5048, NL-2600 GA Delt, Netherlands*

Available online 12 July 2007

Abstract

The area under the load–displacement softening curve gives the total external work on the test specimen and not the fracture energy. The fracture energy follows from half this area that is equal to the critical strain energy release rate at the first crack increment. For wood this is correctly applied for mode II. For mode I however, as for other materials, the total area is wrongly regarded, a factor 2 is too high. In some applications, based on crack increment cycles, the error is even a multiple of this factor 2. On the other hand, the measurements at softening may show an apparent decrease of the specific fracture energy that can be explained by a small crack joining mechanism when the ultimate state of the ligament of the test specimen is reached. Post fracture behaviour is thus not comparable with the behaviour of macro crack initiation.

It is further shown, by the kinetics of the process, that the irreversible work of an ultimate loading cycle is proportional to the activation energy of the fracture process and not to the driving force of the process. This explains why the crack velocity decreases with the increase of this irreversible work and increases with the stress intensity increase.

The fracture energy is a function of the Griffith strength and is thus related to the effective width of the test specimen and not to the ligament length. This also has to be corrected. Based on the derivation of the softening curve, the reported fracture toughness of $720 \text{ kN m}^{-1.5}$ of double-edge notched tests is corrected to $330 \text{ kN m}^{-1.5}$ and the value of $467 \text{ kN m}^{-1.5}$, based on the fracture energy, of the compact tension tests, is also corrected to the right value of $330 \text{ kN m}^{-1.5}$. A revision of published mode I data, based on the fracture energy obtained by the area of the softening curve, is thus necessary.

© 2007 Elsevier Ltd. All rights reserved.

Keywords: Fracture mechanics; Fracture energy; Energy release rate; Softening behaviour; Crack velocity; Molecular fracture kinetics

1. Introduction

The analysis followed here is not based on the singularity approach, thus on stresses at a distance of the singularity, but on determining the ultimate stresses at the crack boundary. Further, wood and other orthotropic materials should be regarded as

reinforced materials. The applied orthotropic Airy stress functions are based on the spread out of the reinforcement to act as a continuum, satisfying the equilibrium, compatibility and strength conditions. In reality only this can be achieved by the interaction through the matrix and the orthotropic solution is thus not right for reinforced materials because the equilibrium conditions and the strength criterion of the matrix, as a determining element, then are not satisfied. This is corrected in [1] by applying the Airy

* Tel.: +31 152851980.

E-mail address: vanderp@xs4all.nl

Nomenclature

A	area; the index indicates a closed curve $A_{OAB} = A_{OABO}$	R	gas constant
a	crack length; $a_{ij} = \text{constant}$	r_0	radius of the crack boundary
b	specimen width	T	absolute temperature
b_{eff}	effective specimen width	t	time, or thickness
C	constant	v	displacement
c	half a crack length; $c_{ij} = \text{constant}$	W	strain energy increase
c_c	critical length of crack c	$\alpha, \beta, \gamma, \eta$	constants
E	elastic modulus	δ	displacement
E_{eff}	elastic modulus of a plate containing a crack	ε	strain
E'	activation energy	ε_g	strain at the Griffith stress on the yield locus
G	energy release rate	λ	jump of the activated segment
G_{xy}	modulus of rigidity	σ	stress
G_C	critical energy release rate	σ_c	cohesive stress or yield stress in MPa
K	stress intensity factor	σ_g	Griffith yield stress
K_C	critical stress intensity factor	σ_r	real mean stress in the determining weakest cross section
K_I	mode I stress intensity factor	σ_t	real local tensile strengths at the crack boundary
l	length of the specimen	ν	contraction coefficient
N	number of fracture sites		

stress function for the stresses in the isotropic matrix giving the right general solution identical to the empirical mixed mode Wu-failure criterion for wood, concrete and fiber reinforced plastics, that is, written in mode I and II stress intensities

$$K_I/K_{Ic} + (K_{II}/K_{IIc})^2 = 1, \quad (1)$$

where K_{IIc} is proportional to K_{Ic} according to Eq. (A.10) of the Appendix.

From the derivation in [1] follows that there is always enough energy for the fracture, but also that the stress should be high enough for failure. Thus the critical fracture energy equation is identical to the failure condition as is shown in [1] and in the Appendix. In Appendix it is also shown that Eq. (1) is an extension and a special case of the SED criterion, e.g. given in [2].

Because of the initial fracture of the isotropic matrix in [3] the derived orthotropic relations between the fracture energy and the mode I and II stress intensities do not apply and do not fit to the measurements of, e.g. [4]. The isotropic relations apply for the strength of the matrix and the matrix stresses determine the stresses of the reinforcement and by that the external loading.

There is also no need for simulation of the steepest stress gradient [5], because the direction of crack

extension is already known from the critical stress state providing the lower bound solution that is based on the (physical possible) flat elliptical crack [1]. For mode I, regarded here because of the necessary correction of the fracture energy, the initial crack and crack extension are both in the grain direction, but the following derivation is comparable for mode II and the mixed mode [1].

2. Fracture energy, strain energy and energy release rate

The mode I fracture energy, measured by the specimen of Fig. 1, is stated to be equal to the area under the softening curve of Figs. 2, 3, 6 or 7, divided by the total crack area and thus is stated to be equal to the total work at fracture done by the external forces on the specimen. This is not right. It is half this value as will be shown here and in paragraph 4. In paragraph 4, it is shown that the fracture energy of mode II of wood is correctly based on half the area under the non-linear part of the loading diagram and also that the critical strain energy release rate, applying at the top of the loading curve, at the start of softening, is correctly in agreement with the area method, accounting half the incremental area of this curve according to the

energy balance. The factor 2 error in the mode I fracture energy explains why in the RL and TL direction, the fracture energy of wood is twice the critical strain energy release rate as is mentioned as general empirical property in [6, p. 114].

As most materials, wood shows near failure an apparent plastic behaviour and the loading curve can be approximated by equivalent elastic–plastic behaviour. Therefore linear elastic fracture mechanics can be applied based on the ultimate stress at the elastic–plastic boundary around the crack tip. The dissipation by microcracking, plastic deformation and friction within this boundary, called fracture process zone, can then be seen as parts of the fracture energy of the macro crack extension. The linear elastic derivation of the softening curve, given in paragraph 3, shows that the critical strain energy release rate is equal to the specific fracture energy as long as the ligament length is not determining.

In the literature, the derivation of Eq. (6) is based on the reciprocal theorem. However, the following derivation more clearly shows the essence of the fracture energy and the energy exchanges.

In Fig. 1, a mode I, center notched test specimen is given with a length “ l ”, a width “ b ” and thickness “ t ”, loaded by a stress σ showing a displacement δ of the loaded boundary due to a small crack extension. The work done by the constant external stress σ on this specimen during this crack extension is equal to

$$2W = \sigma \cdot b \cdot t \cdot \delta, \quad (2)$$

twice the increase of the strain energy W of the specimen so that the other half of the external work,

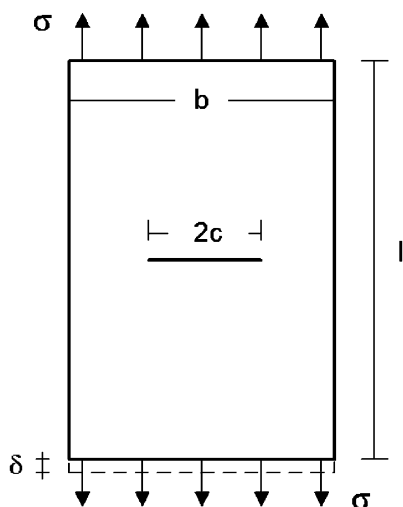


Fig. 1. Specimen b times l with thickness t , containing a flat crack of $2c$.

equal to the amount W , is the fracture energy, used for crack extension. Thus the fracture energy is equal to half the applied external energy that is equal to the strain energy increase W and follows for the total crack length from the difference of the strain energy of a body containing the crack and of the same body without a crack

$$\frac{\sigma^2}{2E_{\text{eff}}} b l t - \frac{\sigma^2}{2E} b l t = W. \quad (3)$$

The fracture energy is also equal to the strain energy decrease at fixed grip conditions when $\delta = 0$

$$W = t \sigma \int_{-c}^{+c} v da = \pi \sigma^2 c^2 t / E, \quad (4)$$

where the last two terms give the strain energy to open (or to close) the flat elliptical crack of length $2c$ and where “ v ” is the displacement in the middle of the crack surface in the direction of σ (see [1]).

From Eqs. (3) and (4) it follows that:

$$\frac{\sigma^2}{2E_{\text{eff}}} b l t - \frac{\sigma^2}{2E} b l t = \pi \sigma^2 c^2 t / E. \quad (5)$$

Thus the effective Young’s modulus of the specimen of Fig. 1 containing a crack of $2c$, is

$$E_{\text{eff}} = \frac{E}{1 + 2\pi c^2 / b l}. \quad (6)$$

It follows from the kinetics of crack propagation that the critical crack length is in an unstable equilibrium. Thus for a crack length $2c$ in a material of thickness t , the condition of unstable equilibrium is

$$\frac{\partial}{\partial c} (W - G_c 2ct) = 0, \quad (7)$$

where G_c is the fracture energy for the formation of the crack surface per unit crack area. Because $G_c = \partial W / \partial (2ct)$, it clearly also is a strain energy release rate when applied to Eq. (4). With W of Eq. (3) or of Eqs. (4), (7) becomes

$$\frac{\partial}{\partial c} \left[\frac{\pi \sigma^2 c^2 t}{E} - G_c 2ct \right] = 0,$$

$$\text{or } \frac{\partial}{\partial c} \left[\frac{\sigma^2 b l t}{2E} \left(1 + \frac{2\pi c^2}{b l} \right) - \frac{\sigma^2 b l t}{2E} - G_c 2ct \right] = 0$$

giving both the Griffith strength

$$\sigma_g = \sqrt{\frac{G_c E}{\pi c}}. \quad (8)$$

This stress is related to the width b of the specimen of Fig. 1. The real mean stress in determining the

weakest cross section with width $b-2c$, where fracture occurs is

$$\begin{aligned}\sigma_r &= \sqrt{\frac{G_c E}{\pi c}} \cdot \frac{b}{b-2c} \\ &= \sqrt{\frac{G_c E}{\pi b}} \cdot \frac{1}{(\sqrt{c/b}) \cdot (1-2c/b)}\end{aligned}\quad (9)$$

and

$$\frac{\partial \sigma_r}{\partial (\sqrt{c/b})} = \sqrt{\frac{G_c E}{\pi b}} \cdot \frac{6c/b - 1}{(c/b) \cdot (1-2c/b)^2} > 0,$$

when $c/b > 1/6$,

that always is the case for critical crack lengths and the real stress σ_r increases monotonically with the increase of the crack length c and no softening behaviour exists at the critical site. Softening thus only exists outside the critical cross section and is identical to elastic unloading of the specimen outside the fracture zone and thus also in this case, softening is not a material property as is assumed in the existing models for wood and concrete.

3. The strain softening curve

A simple description of the softening behaviour as a result of former crack propagation alone is possible by the Griffith theory. Straining the specimen of Fig. 1 to the ultimate load at which the initial crack will grow, gives according to Eq. (6): $\varepsilon_g = \sigma_g / E_{\text{eff}} = \sigma_g \cdot (1 + 2\pi c^2/bl) / E$.

Substitution of $c = G_c E / \pi \sigma_g^2$, according to Eq. (8), gives

$$\varepsilon_g = \sigma_g / E + 2G_c^2 E / \pi \sigma_g^3 bl. \quad (10)$$

This is the equation of critical unstable equilibrium states should therefore apply along the softening curve (for a sufficiently long ligament length of the test specimen). This curve, called Griffith locus, has a vertical tangent $d\varepsilon_g/d\sigma_g = 0$, occurring at a crack length of

$$c_c = \sqrt{bl/6\pi}. \quad (11)$$

Cracks smaller than $2c_c$ are unstable because of the positive slope of the locus. These cracks extend during the loading stage, by the high peak stresses at the notch of the test specimen, to a stable length and only crack lengths higher than c_c are to be expected at the highest stress, giving the stress–strain curve of Fig. 4 with σ_c as a top value (or σ_c randomly above the top value of the real curve).

For a distribution of small cracks, b and l in Eq. (11) are the crack distances and the critical crack distance for extension is about 2.2 times the crack length; this occurs when $b \approx 2.2 \cdot 2c_c$ and $l \approx 2.2 \cdot 2c_c$, or $bl \approx 19 \cdot c_c^2 \approx 6\pi c_c^2$. This critical distance is predicted by deformation kinetics [7] and is used in paragraph 8.

According to Eq. (10), the softening line can now be given as

$$\varepsilon_g = \frac{\sigma_g}{E} \left(1 + \frac{\sigma_c^4}{3\sigma_g^4} \right), \quad (12)$$

where

$$\sigma_c = \sqrt{EG_c/\pi c_c} \quad (13)$$

is the ultimate load with c_c according to Eq. (11). The negative slope of this softening line is

$$\frac{\partial \sigma_g}{\partial \varepsilon_g} = -\frac{E}{\frac{\sigma_c^4}{\sigma_g^4} - 1} = -\frac{E}{\frac{\varepsilon_c^2}{\varepsilon_g^2} - 1}. \quad (14)$$

A vertical yield drop occurs at the top at $\sigma_g = \sigma_c$, and the strain then is: $\varepsilon_{gc} = (\sigma_c/E) \cdot (1 + 1/3)$ and Eq. (12) becomes

$$\frac{\varepsilon_g}{\varepsilon_{gc}} = 0.75 \cdot \left(\frac{\sigma_g}{\sigma_c} + \frac{\sigma_c^3}{3\sigma_g^3} \right). \quad (15)$$

In general Eq. (12) can be written, when related to a stress level σ_{g1}

$$\begin{aligned}\frac{\varepsilon_g}{\varepsilon_{g1}} &= \frac{\sigma_g}{\sigma_{g1}} \cdot \frac{1 + \sigma_c^4/3\sigma_g^4}{1 + \sigma_c^4/3\sigma_{g1}^4} \\ &= \frac{\sigma_g}{\sigma_{g1}} \cdot \frac{1 + (\sigma_c/\sigma_{g1})^4 \cdot (\sigma_{g1}/\sigma_g)^4/3}{1 + (\sigma_c/\sigma_{g1})^4/3}.\end{aligned}\quad (16)$$

To control whether σ_c changes, Eq. (16) can be written as

$$\frac{\sigma_c}{\sigma_{g1}} = \left(\frac{3 \cdot (\sigma_g/\sigma_{g1})^3 \cdot ((\varepsilon_g/\varepsilon_{g1}) - (\sigma_g/\sigma_{g1}))}{1 - (\varepsilon_g/\varepsilon_{g1}) \cdot (\sigma_g/\sigma_{g1})^3} \right)^{0.25} \quad (17)$$

with the measured values on the right hand side of the equation. When σ_c decreases, the mechanism discussed in paragraph 8 is determining for softening and the value of σ_c . However, as an approximation, Eq. (15) can also be applied with a stepwise decrease of σ_c , as is discussed in paragraph 8.

Applications of the Griffith locus can be found in numerous publications in the past, e.g. in [5], where it is used as a failure criterion for the onset of unsta-

ble crack growth. Here it is shown that the stable part of the locus should represent the softening curve. It will be further shown that the occurring softening curve may differ from the Griffith locus and may be steeper due to the crack joining mechanism discussed in paragraph 8.

4. Fracture energy as area under the softening curve

The basic theory of the energy method, leading to Eqs. (2) and (3), should be confirmed by the loading curve (Fig. 2). This will be discussed in the following.

When a test specimen is mechanically conditioned, the effective stiffness is obtained given by the lines OA and OC in Figs. 2 and 3. In Fig. 2, the area OAB, written as A_{OAB} , is the strain energy of the specimen of Fig. 1 with a central crack (or

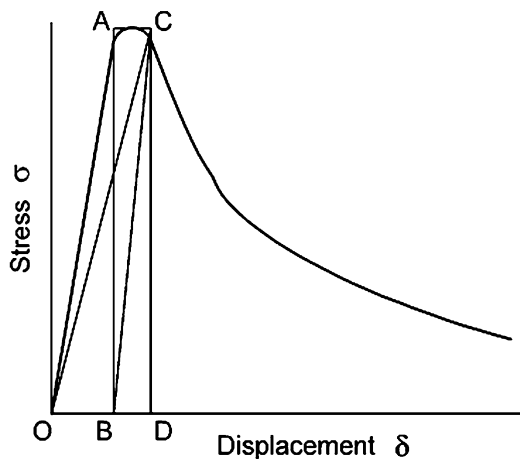


Fig. 2. Stress–displacement curve for tension of the specimen of Fig. 1 or 5.

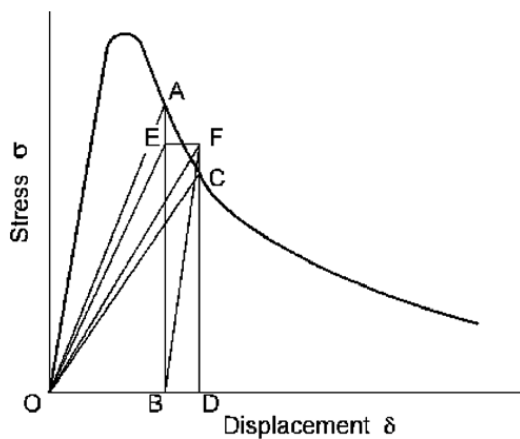


Fig. 3. Descending branch of the stress–displacement curve of Fig. 2.

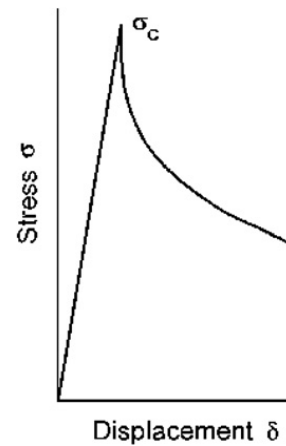


Fig. 4. Softening curve according to Eq. (10) for the specimen of Fig. 1 or 5.

with two side cracks according to Fig. 5) with a width “ b ”, length “ l ” and thickness “ t ” loaded to the stress σ . During the quasi static crack extension from B to D in Fig. 2, the constant external load σ does the work on the specimen of

$$\sigma \cdot b \cdot t \cdot \Delta \varepsilon_{BD} \cdot l = \sigma \cdot b \cdot t \cdot \delta_{BD} = A_{ABDC},$$

where $\Delta \varepsilon_{BD}$ is the strain increase due to the cracking and δ_{BD} the corresponding displacement. The strain energy after the crack extension is A_{OCD} and the strain energy increase by the crack extension is thus shown in Fig. 2

$$A_{OCD} - A_{OAB} = A_{OCD} - A_{OCB} = A_{CBD} = A_{ABDC}/2.$$

Thus half of the external energy $\sigma \cdot b \cdot t \cdot \delta_{BD}/2$ is the amount of increase of the strain energy due to the elongation by δ , and the other half is thus the fracture energy that is equal to this increase of strain energy.

The same follows at unloading at yield drop. Because every point of the softening curve gives the Griffith strength, which decreases with increasing

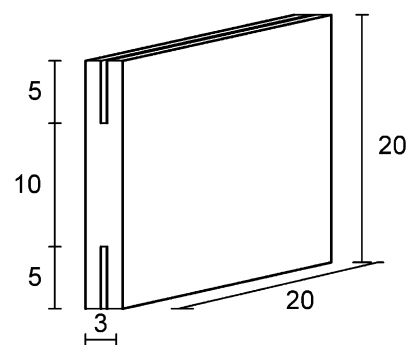


Fig. 5. Geometry of the specimens [4].

crack lengths, unloading is necessary to maintain equilibrium. The fracture with unloading step AC in Fig. 3 is energy equivalent to the unloading steps AE and FC and the fracturing step EF at constant stress $EB = FD = (AB + DC)/2$. Thus $A_{ABDC} = A_{EBDF}$. Identical to the first case of Fig. 2, the increase in strain energy due to crack extension is

$$\begin{aligned} A_{ODF} - A_{OBE} &= A_{ODF} - A_{OBF} = A_{BFD} \\ &= 0.5 \cdot A_{EBDF} = 0.5 \cdot A_{ABDC}, \end{aligned}$$

equal to half the work done by the external stresses during crack propagation and thus also equal to the other half, the work of crack extension. The derivation further shows that there is more energy available than necessary for fracture as also found in [1], mentioned in paragraph 1. The conclusion is that not the total area under the load–displacement curve, divided by the corresponding total crack length (including the initial length), is equal to the specific fracture energy, but only half this area. The published mode I values of the so-determined fracture energies thus need to be corrected. This is not the case for mode II. In the same way as for mode I, half the area under the non-linear part of the loading diagram is equal to the fracture energy for mode II. For this mode, only line OACO in Fig. 2 is measured and A_{OAC} is regarded to be the fracture energy. Because $A_{OAC} = A_{BAC} = 0.5 \cdot A_{ABDC}$, this is right and mode II needs no correction.

5. Necessary corrections of the fracture energy

As shown above, the area under the load–displacement curve is equal to the work done by the external stresses and half this work is used for fracture.

Thus for the extension BD in Figs. 2 and 3, the fracture energy ($A_{ABDC}/2$ or $A_{EBDF}/2$) is at constant stress σ (AB or EB)

$$\begin{aligned} \sigma \cdot b \cdot t \cdot \delta_{BD}/2 &= \sigma \cdot b \cdot t \cdot l \cdot \Delta\epsilon/2 \\ &= \frac{\sigma^2 \cdot b \cdot t \cdot l}{2} \\ &\cdot \left(\frac{1}{E} \cdot \left(1 + \frac{(c + \Delta c)^2}{3 \cdot c_c^2} \right) - \frac{1}{E} \cdot \left(1 + \frac{c^2}{3 \cdot c_c^2} \right) \right) \\ &= \frac{\sigma^2 b t l}{2E} \cdot \frac{2c\Delta c}{3c_c^2} = \frac{\sigma^2 b t l 6\pi c \Delta c}{3E b l} \\ &= \frac{\sigma^2 t 2\pi c \Delta c}{E}. \end{aligned} \tag{18}$$

This is equal to the increase of fracture energy at crack extension of $\Delta(G_c \cdot t \cdot 2c) = 2 \cdot G_c \cdot t \cdot \Delta c$. Thus, $\sigma^2 t 2\pi c/E = 2G_c t$, or: $\sigma_g = \sqrt{EG_c/(\pi c)}$, equal to the Griffith strength and thus showing that the fracture energy G_c is equal to the energy release rate. Thus it is now shown that half the area $A_{ABDC}/2$ is equal to the fracture energy and not the whole area and it is also shown that the totally different amount A_{OACO} of Fig. 3 is not equal to the fracture energy, as is supposed in [8] for crack increments (see paragraph 6).

Because Eq. (3) is based on the total crack length and the strength is a Griffith stress, the initial value $2c$ of the crack length should be accounted for and σ and G_c should be related to the whole crack length, including the initial value, and thus should be related to the whole specimen width b and not to the reduced width of the ligament: $b-2c$ as is done now. This is the second necessary correction of the mode I fracture energy G_c .

A third correction is necessary when σ_c of Eq. (12) changes. Then Eq. (18) becomes

$$\begin{aligned} \sigma \cdot b t \delta_{BD}/2 &= \frac{\sigma^2 b t l}{2} \cdot \left(\frac{1}{E} \cdot \left(1 + \frac{(c + \Delta c)^2}{3 \cdot (c_c + \Delta c_c)^2} \right) - \frac{1}{E} \cdot \left(1 + \frac{c^2}{3 \cdot c_c^2} \right) \right) \\ &= \Delta(G_c t 2c) = G_c t 2 \cdot \Delta c + t 2c \cdot \Delta G_c, \\ \text{or: } \frac{\sigma^2 \pi c}{E} \left(1 - \frac{\Delta c_c}{c_c} \cdot \frac{c}{\Delta c} \right) &= G_c + \frac{\Delta G_c \cdot c}{\Delta c} \\ \text{or: } \frac{\Delta G_c}{G_c} &= -\frac{\Delta c_c}{c_c} = -\Delta \ln(c_c). \end{aligned} \tag{19}$$

Thus the apparent decrease of the energy release rate ΔG_c is proportional to $\Delta \ln(c_c)$. The apparent value of G_c may decrease at the end of the fracture process, when the ligament strength of the test specimen becomes determining, due to the small crack extension, reducing the ligament area of the specimen. This is discussed in paragraph 8. The measurements of [4], on the test specimens of Fig. 5, show a strong influence of this ligament fracture mechanism and there thus is a difference between this specific fracture energy of the post fracture state and the strain energy release rate of crack initiation based on the ultimate Griffith strength at the top of the softening curve.

6. Irreversible work of an ultimate loading cycle

The irreversible energy of a loading cycle with a crack increment on a test specimen is given by the triangle A_{OACO} in Fig. 3. The superfluous elastic unloading parts, not needed for the fracture energy

calculation are A_{OEA} and A_{OCF} and the fracture energy is given by the area A_{OEF} . In [8], A_{OACO} is measured, at different crack velocities, for a range of crack increments on the same specimen. The area of $A_{OACO} = A_{OEF} + (A_{OAE} + A_{OCF})$ or

$$A_{OACO} = \sigma \cdot btl \cdot \Delta\varepsilon/2 + |\Delta\sigma| \cdot btl \cdot \varepsilon = \frac{\sigma \cdot btl \cdot \Delta\varepsilon}{2} \left(1 + \left| \frac{\Delta\sigma}{\Delta\varepsilon} \right| \cdot \frac{\varepsilon}{\sigma} \right).$$

Inserting Eqs. (12) and (14) gives

$$A_{OACO} = \frac{\sigma^2 t 2\pi c \Delta c}{E} \left(1 + \left(1 + \frac{\sigma_c^4}{3\sigma^4} \right) \cdot \left(\frac{1}{\sigma_c^4/\sigma^4 - 1} \right) \right) = \frac{\sigma^2 t 2\pi c \Delta c}{E} \cdot \frac{4/3}{1 - (\sigma/\sigma_c)^4}.$$

This area is supposed to be equal to an apparent fracture energy $G_{c,a}$. It is already shown that the first term is equal to the Griffith fracture energy G_c according to: $\Delta(G_c t 2c) = 2G_c t \cdot \Delta c$ and thus $G_{c,a}$ is assumed to be proportional to G_c which also applies: $\Delta(G_{c,a} t 2c) = 2G_{c,a} t \cdot \Delta c$, giving

$$G_{c,a} = \frac{\sigma^2 \pi c}{E} \cdot \frac{4/3}{1 - (\sigma/\sigma_c)^4} = G_c \cdot \frac{4/3}{1 - (\sigma/\sigma_c)^4} = G_c \cdot \frac{4/3}{1 - (c/c)^2}. \quad (20)$$

This equation only applies as long as the modified Griffith locus, (Eq. (12)), is followed during softening, thus, maximal to about half the unloading for the specimen of Fig. 5. When the slope of the softening curve at the start fits to $c/c \approx 0.9$, then $G_{c,a} \approx 7 \cdot G_c$. When this is $c/c \approx 0.8$, then $G_{c,a} \approx 3.7 \cdot G_c$. Thus different factors can be measured depending on the steepness of the softening curve at the start. This result demonstrates that $G_{c,a}$ is not the fracture energy but contains, as shown, a superfluous amount of energy for fracture.

As mentioned, depending on the ligament length of the test specimen, a crack joining mechanism, discussed in paragraph 8, may become determining for the softening stage and Eq. (12) then does not apply any more because c_c increases with c and the Griffith G_c decreases because of the decreasing ligament area due to the small crack extension at the ligament. The softening curve is then found by integration of the common damage equation of [7]. This behaviour and the meaning of $G_{c,a}$ will be explained in paragraph 8.

7. Experimental verification

Testing the theory the best can be done by the elementary stress states of the center notched, or double-edge notched specimens. The measurements of [4] are sufficiently complete by measuring the whole loading and softening curve and using the compact tension tests as control, being a control by the different loading case.

The graphs of [4], Figs. 6 and 7, are the result of tension tests on the specimen of Fig. 5. The length of the specimen was $l = 3$ mm, the width and thickness: $b = t = 20$ mm and the notch length $2c = 2 \times 5 = 10$ mm with a notch width of 0.5 mm.

The double-edge notched specimen was used in [4] at the highest moisture content because the single side notched specimen failed at the glued boundaries. Therefore also a shorter ligament length was

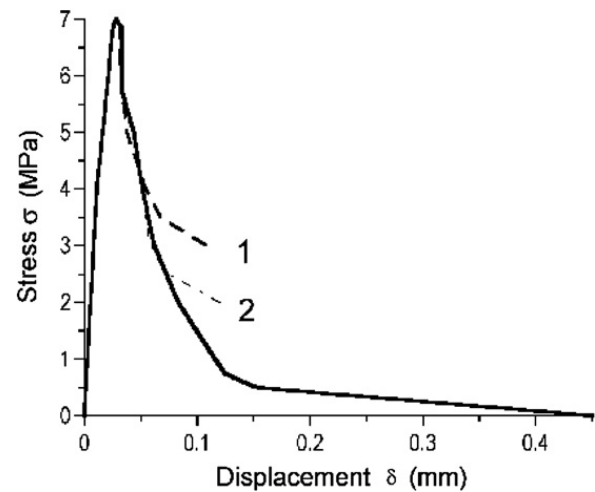


Fig. 6. Stress–displacement of specimen T 1409 of [4].

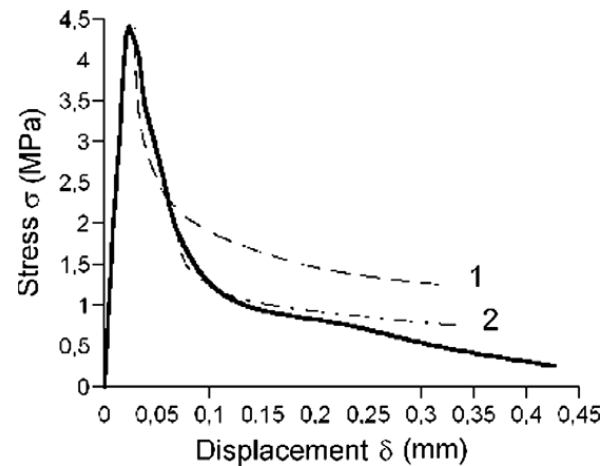


Fig. 7. Stress–displacement of specimen T 1509 of [4].

necessary. However, the ligament strength now becomes determining and also the boundary discontinuity at the glued steel plates still may remain determining as is shown.

In the Figs. 6 and 7, the measured stress–displacement is given together with the lines 1 and 2 according to Eq. (15). The strain ε_g follows from the displacements at the x -axis of the figures divided through 3 mm, the measuring length and length of the specimen. Because of the small length of 3 mm, not the whole width b of the specimen is active. Assuming a possible spreading of 1.2:1, through the thickness of 1.25 mm above and below the side notches, the working width b_{eff} is equal to the ligament length plus two times 1.2×1.25 or $b_{\text{eff}} = 10 + 3 = 13$ mm. Thus the real specimen has the same dimensions as given in Fig. 5, except for the notch lengths that should be regarded to be 1.5 mm instead of 5 mm. The stresses in the Figs. 6 and 7 of [4], are related to the ligament length and not to b_{eff} , according to the Griffith stress. Thus the stresses have to be reduced by a factor $10/13 = 0.77$.

The standard compact tension tests of [4] did show a stress intensity K_{Ic} of $330 \text{ kN m}^{-3/2}$. This result is independent of the chosen stiffness as follows from the calculation according to the series solution or according to the energy method. This is verified in [4] by comparing the series solution with a finite element compliance calculation using the isotropic and the orthotropic stiffness and the orthotropic stiffness of [3]. The value of $K_{Ic} = 330 \text{ kN m}^{-3/2}$, found in all cases, thus also should follow from the area under the softening curve of that compact tension test. When half the area of that diagram is taken to be the fracture energy, instead of the total area, then K_{Ic} , mentioned in [4], indeed is corrected to the right value of: $467/\sqrt{2} = 330 \text{ kN m}^{-3/2}$. This result of the standard compact tension test thus is a first experimental verification of the theory.

Regarding the short double-edge notched specimens of Fig. 5, the measured E-modulus should be related to the effective width of 13 mm instead of the ligament width of 10 mm and therefore is $E = 700 \times 10/13 = 700 \times 0.77 = 539 \text{ MPa}$. The critical energy release rate then is

$$G_c = K_{Ic}^2/E = 330^2/539 = 200 \text{ N/m}. \quad (21)$$

The measured value of G_c from the area under the stress–displacement curve is given in [4] to be 515 N/m . But, because half this area should have

been taken and this value is wrongly related to the ligament length instead of on b_{eff} , the corrected value is: $1/2 \times 515 \times 0.77 = 200 \text{ N/m}$, as found above, Eq. (21), giving again an experimental verification of the theory, now by the tests on the short double-edge notched specimens.

It is seen that the curve of Fig. 6 has a vertical tangent at the top $d\sigma_g/d\varepsilon_g = \infty$. The critical crack length there thus is: $c_c = \sqrt{bl/6\pi}$ according to Eq. (11). Thus

$$c_c = \sqrt{\frac{b_{\text{eff}}l}{6 \cdot \pi}} = \sqrt{\frac{13 \cdot 3}{6 \cdot \pi}} \cdot 10^{-3} = 1.5 \cdot 10^{-3} \text{ m} \\ = 1.5 \text{ mm}. \quad (22)$$

In Fig. 6, at the Griffith maximal stress of $(0.77) \cdot 7 = 5.39 \text{ MPa}$, is: $K_{Ic} = \sigma\sqrt{\pi c}$ or

$$K_{Ic} = 5.39 \cdot \sqrt{\pi \cdot 1.5 \cdot 10^{-3}} = 0.37 \text{ M Nm}^{-3/2}. \quad (23)$$

Line 1 of Fig. 6 gives the primary crack extension, Eq. (15), with $\sigma_c = (0.77) \cdot 7 = 5.39 \text{ MPa}$ and a displacement of about 0.03 mm, or a strain of $0.03/3 = 0.01$. The ligament strength of 7 to 8 MPa is exceptionally high and only measured 6 times of the 117 tests. The crack does not propagate in a free space, but in the limited length of the ligament and this area will be overloaded. Curve 1 therefore levels off from the measurements at $\sigma = 0.77 \cdot 4 \text{ MPa}$. Thus

$$\sigma_g = \sqrt{\frac{EG_c}{\pi 3c_c}} = 0.57 \cdot (0.77 \cdot 7) = 0.77 \cdot 4 \text{ MPa} \quad (24)$$

and the crack length has become about three times the initial critical value $c_{c,0}$. Thus the initial crack of 1.5 mm has traveled two times $1.5 \text{ mm} = 3 \text{ mm}$ and the intact part of the ligament is $10 - 3 = 7 \text{ mm}$. Only one of the 2 side notches is extended, (probably by a high local strength due to crossing ray cells). When both notches extend 1.5 mm, the same intact ligament length of 7 mm occurs and

$$\sigma_g = \sqrt{\frac{EG_c}{\pi 2c_c}} = 0.77 \cdot 4.9 \text{ MPa}. \quad (25)$$

Corrected by the measured $\sqrt{EG_c}$ values of 600/640 to the mean value of the series, this stress becomes $\sigma_g = 0.77 \cdot 4.9 \cdot (600/640) = 0.77 \cdot 4.6 \text{ MPa}$. (26)

This higher value of 4.6 instead of 4, shows the higher strength that is possible when the extensions from both sides are not in the same plane. The level above 4 (to 4.6) MPa is measured in 3 of the 10 specimens of the discussed series T1309/2309 of [4] and an

of a gradual decrease. It should be remarked that the extreme strong specimen of Fig. 6, due to non-comparable, one sided, crack propagation, should be omitted from the data. Further, the lowering of the data line below line 2 in Fig. 7 is due to an increase of the applied strain rate by a factor 7.

The analysis above shows that in general

$$2c_{n+1} = 2 \cdot 2c_n + 2c_0, \text{ giving } 2c_1 = 6c_0 \text{ and} \\ 2c_2 = 2 \cdot 2c_1 + 2c_0 = 14c_0.$$

The increase of the crack length is: $\Delta(2c)' = 2c_{n+1} - 2c_n = 2c_n + 2c_0$. Including the initial crack length of $2c_0$, the increase of the total crack length is

$$\Delta(2c) = 2c_{n+1} - 2c_n - 2c_0 = 2c_n. \quad (27)$$

More general for any crack distance this is: $\Delta(2c) = \beta_1 \cdot 2c$ and because the strength decrease is proportional to the area decrease of the ligament area of the test specimen, due to small cracks extension there, the equation becomes

$$\Delta(2c)/(2c) = -\beta_2 \cdot \Delta(G_c) \quad (28)$$

comparable to Eq. (19), giving the explanation of the decrease of σ_c .

Eq. (28) can also be expressed in the mean crack velocities by replacing c by $\dot{c} \cdot t$, the mean crack velocity \dot{c} times time t . Thus: $\Delta(2c)/(2c) = \Delta(\dot{c}t)/\dot{c}t = \Delta\dot{c}/\dot{c}$. Then integration of Eq. (28) leads to

$$G_{c,a} = G_{c,a,1} - \gamma \cdot \ln(\dot{c}). \quad (29)$$

This is measured in [8] for the irreversible work of loading cycles. Measured are two processes. One with a small slope γ , and one with a high value of γ . The slope γ is small for crack velocities \dot{c} above 2.4 mm/s and is high below this velocity. For instance in the RL direction, at crack velocities between $\dot{c} = 0.2$ to 2.4 mm/s, is found

$$G_{c,a} = 258 - 150 \cdot \ln(\dot{c}), \quad (30)$$

running from $G_{c,a} = 500$ N/m at 0.2 mm/s to $G_{c,a} = 126$ N/m at 2.4 mm/s. However, from other slow crack growth investigations, only the high crack velocity process of [8] with the small value of γ is found as, e.g. is shown in [9]. Further, in the overlapping range of 0.01 mm/s to 1 mm/s, no decrease, but an increase of the stress intensity K_I , thus of $\sqrt{G_c}$, is measured. This can be explained as follows. Eq. (29) can also be written

$$\dot{c} = \dot{c}_0 \cdot \exp\left(-\frac{E' - \sigma_t \lambda / N}{RT}\right), \quad (31)$$

where \dot{c}_0 is the maximal value of \dot{c} ; E' the activation energy, containing the enthalpy and entropy terms; $\sigma_t \lambda / N$ the work term by the stress σ_t on the site [7]; R the gas constant and T the absolute temperature.

Eq. (31) is a special case of the general damage equation of softening of [7], that applies because mean rates \dot{c} of the crack increments are regarded. This equation can be related to a reference value \dot{c}_1

$$\ln(\dot{c}) = \ln(\dot{c}_1) - (E' - \sigma_t \lambda / N) / RT \\ + (E' - \sigma_{t,1} \lambda / N_1) / RT \quad (32)$$

For $\dot{c}_1 = 1$ mm/s, it follows from Eqs. (29) and (32) that

$$G_{c,a} / \gamma = (E' - \sigma_t \lambda / N) / RT \quad (33)$$

and it is seen that $G_{c,a}$, the irreversible work of an ultimate loading cycle, discussed in paragraph 6, is proportional to the apparent activation energy of the process and is not the driving force of the process. $G_{c,a}$ decreases with the increase of the driving force σ_t . Therefore the crack velocity decreases with the increase of $G_{c,a}$ because the driving force σ_t decreases. According to Eq. (30) is measured: $G_{c,a} / \gamma = 258 / 150 = 1.72$, that means $\sigma_{t,1} \lambda / RTN_1$ is close to E' / RT at fracture because these terms are much higher than 1.7. The high value of γ and the small influence of the moisture content on the slope and the shift of the curve indicates that this process is a mechanosorptive process [7]. This probably is due to the moisture transport during the testing due to the other climatic conditions than those of the conditioned specimens. The testing should be repeated at constant climate conditions for verification.

Eq. (32) also can be written as

$$\ln(\dot{c}) = \ln(\dot{c}_1) + \sigma_t \lambda / NRT - \sigma_{t,1} \lambda / N_1 RT, \quad (34)$$

and measurements show that the number of sites N is proportional to the applied stress σ_t and the initial value of N thus is proportional to the ever applied maximal stress $\sigma_{t,m}$. This is a property of many materials that explains, e.g. the time–stress equivalence found in [7]. In Eq. (34) thus is $\sigma_{t,m} / N = \sigma_{t,1} / N_1$ and Eq. (34) becomes $n = \sigma_{t,1} \lambda / N_1 RT = \sigma_{t,m} \lambda / NRT$

$$\ln(\dot{c}) = \ln(\dot{c}_1) + n \cdot \sigma_t / \sigma_{t,m} - n, \quad \text{or} \\ \frac{\sigma_t}{\sigma_{t,m}} = 1 + \frac{1}{n} \ln\left(\frac{\dot{c}}{\dot{c}_1}\right) \quad (35)$$

showing the increase of the crack velocity \dot{c} with the increase of σ_t . By multiplication of the local tensile strengths at the crack boundary σ_t and $\sigma_{t,m}$ with

$\sqrt{2\pi r_0}$, according to [1], the equation is expressed in the mean stress σ in the specimen because $\sigma_{t,m}\sqrt{2\pi r_0} = \sigma\sqrt{\pi c} = K_I$, and Eq. (35) becomes

$$\frac{K_I}{K_{I,1}} = 1 + \frac{1}{n} \ln\left(\frac{\dot{c}}{\dot{c}_1}\right) = 1 + \frac{1}{n'} \log\left(\frac{\dot{c}}{\dot{c}_1}\right), \quad (36)$$

where n' is in the order of 60 for wood. This is high enough for the possibility of primary C–C- and C–O-bond breaking. The semi log-plot, Eq. (36), is given, as empirical line, in many publications from experiments on ceramics, polymers, metals and glasses and is given in [9] for wood. Because the slope is small, also the empirical double log-plot is possible.

The kinetics shows the same behaviour as for clear wood. As shown in [7], two coupled processes act, showing the same time–temperature and time–stress equivalence. One process, with a very high density of sites, provides the sites of the second process with a very low density, as follows from a very long delay time. The notched specimen discussed here also shows the low concentration reaction by the strong softening behaviour. The concentration here consists of only one initial crack or two crack tips. In the critical cross section through this notch, however, there is no softening and here the determining high concentration reaction acts as follows from Eqs. (30) or (36). Probably numerous small cracks grow to the macro notch, providing the site for the macro crack to grow. This failure mechanism thus applies for every bond breaking process at any level. Even Eq. (1), written in stresses, applies for clear wood as follows from the polynomial description of the failure criterion [10].

9. Conclusions

- A derivation of the softening curve is given based on small crack extensions joining the crack tip of the initial notch of the test specimen. The softening curve follows at the start the stable part of the Griffith locus. This means that every point of the softening curve gives the Griffith strength. This curve, Eqs. (15) or (16), depends on only one parameter, the maximal critical Griffith stress σ_c and thus depends on the critical crack length, Eq. (13), or critical crack density, Eq. (11). For the double-edge notched test specimens of [4], the curve applies until half way to the unloading. Then the ligament strength of the test specimen becomes determining which can be precisely explained by a crack joining mechanism, chang-

ing the crack density and intact ligament area by the limited ligament area and therefore causing a decrease of σ_c and an apparent decrease of the fracture energy.

- The fracture energy for mode I is stated in literature to be equal to the area under the softening curve divided through the total crack length. This is not right. It is shown here that half this area has to be accounted. This already is applied and accepted for mode II in wood.
- It also is stated that the irreversible energy of an ultimate loading cycle, given by the triangle A_{OACO} in Fig. 3, divided by the area of the crack increment, is equal to the fracture energy. This also is not right. It is shown here that this energy is proportional to the apparent activation energy of the fracture process. This explains why the crack velocity decreases with the increase of this energy, while the reverse is the case for the fracture energy given by K_I in Eq. (36).
- Softening is a matter of elastic unloading of the specimen outside the fracture zone. The real mean stress in determining the weakest cross section containing the crack, where fracture occurs, increases with the increase of the crack length. Softening thus is not a material property.
- The softening curve can be approximated by Eq. (15) at the start until half the strength value and then again applying Eq. (15) at half the strength value.
- The standard compact tension tests of [4] indicated a stress intensity K_{Ic} of $330 \text{ kN m}^{-3/2}$. When the theoretically correct value of half the area under the stress–displacement line of these compact tension tests is taken to be the fracture energy, instead of the total area, then the hereupon based value of K_{Ic} is corrected to the right value of: $467/\sqrt{2} = 330 \text{ kN m}^{-3/2}$.
- The problem of [4] is solved of recording on double-edge notched specimens, a K_{Ic} of $720 \text{ kN m}^{-3/2}$, that is more than twice the value of $330 \text{ kN m}^{-3/2}$ of the compact tension tests. This is explained as follows: The given orthotropic correction does not apply for wood [1]. From the measured E and energy G_c follows: $K_{Ic} = \sqrt{E \cdot G_c} = \sqrt{700 \cdot 515} = 600 \text{ MPa}$ instead of $720 \text{ kN m}^{-3/2}$. However, the measured E -modulus should be related to the effective width of about 13 mm instead of the ligament width of 10 mm and therefore is: $E = 700 \times 0.77 = 539 \text{ MPa}$. The measured critical energy release rate or fracture energy, measured from the

area under the stress–displacement curve, should be based on half this area and also on b_{eff} instead of the ligament length and the given value of 515 N/m should be corrected to: $1/2 \times 515 \times 0.77 = 200$ N/m. Then $K_{\text{Ic}} = \sqrt{E \cdot G_c} = \sqrt{539 \cdot 200} = 330 \text{ kN m}^{-3/2}$, as should be according to the compact tension tests.

- A revision of all published mode I data of the fracture energy, based on the area of the softening curve, is necessary. This area method, that shows the post fracture behaviour and not the Griffith strength of crack extension, should not be used anymore. A right description follows from the apparent energy release rate based on the measured strength.
- The kinetics of the cracking process throws a new light on the explanation of strength behaviour.

Appendix

Fracture mechanics of wood is normally restricted to fracture along the grain. It is not possible to have shear crack propagation across the grain. Also the mixed mode crack follows the weak material axes and only may periodically jump to the next growth layer at a weak spot. Applying the SED criterion of Sih, Eq. (A.1), as fracture criterion for a crack in these planes of symmetry, the factor $a_{12} = 0$ because of the, by symmetry forced, zero angle of crack extension. Thus

$$S = a_{11}K_I^2 + 2a_{12}K_I K_{II} + a_{22}K_{II}^2 \quad (\text{A.1})$$

becomes

$$S = a_{11,0}K_I^2 + a_{22,0}K_{II}^2. \quad (\text{A.2})$$

This equation now is the critical energy equation for the determining fracture of the isotropic matrix. The reinforcement of wood acts only in the crack direction and does not affect mode I, but does act as a shear reinforcement. Thus for the stresses in the reinforcement, K_{II} has to be multiplied by a factor η in proportion to the moduli of elasticity of reinforcement and matrix [1].

For wood and some other materials there is a different strength behaviour for tension and compression and accounting for that in one equation leads to Eq. (A.3), of a shifted curve along the K_I -axis.

$$S' = a_{11,0}(K_I + K_{I,0})^2 + a_{22,0}\eta^2 K_{II}^2. \quad (\text{A.3})$$

This equation applies for small crack extension of “clear” wood in the tangential plane. Eq. (A.3) can be written in the form of

$$1 = c_1 K_I + c_{11} K_I^2 + c_{22} K_{II}^2 \quad (\text{A.4})$$

that also can be read in stresses as failure criterion. It is shown in [10], that the general second order tensor polynomial may represent a critical energy criterion for failure while higher order terms are due to hardening and toughening. Wood and some other materials show such behaviour by the increase of the shear strength with compression perpendicular to the crack plane according to the higher order coupling term $3c_{122}K_I K_{II}^2$ and then now failure after some toughening is regarded as the ultimate state, the critical energy equation becomes

$$1 = c_1 K_I + c_{11} K_I^2 + c_{22} K_{II}^2 + 3c_{122} K_I K_{II}^2. \quad (\text{A.5})$$

This equation can be written

$$\left(\frac{K_{II}}{K_{IIc}}\right)^2 = \frac{\left(1 - \frac{K_I}{K_{Ic}}\right) \cdot \left(1 + \frac{\alpha K_I}{K_{Ic}}\right)}{1 + \frac{C\alpha K_I}{K_{Ic}}} \approx 1 - \frac{K_I}{K_{Ic}} \quad (\text{A.6})$$

identical to Eq. (1) of the main section paragraph 1, because $C \approx 0.99 \approx 1$.

The term

$$\left(1 + \frac{\alpha K_I}{K_{Ic}}\right) / \left(1 + \frac{C\alpha K_I}{K_{Ic}}\right) \approx 1 \quad (\text{A.7})$$

for $C = 0.99$ gives a sharp cut off of the parabolic Eq. (A.8) at the compression strength perpendicular to the grain and thus only is noticeable very close to this compression strength. Thus Eq. (A.8) applies generally for mixed mode fracture of wood and comparable materials

$$\left(\frac{K_{II}}{K_{IIc}}\right)^2 = 1 - \frac{K_I}{K_{Ic}}. \quad (\text{A.8})$$

In Eq. (A.6) is $\alpha = \sigma_{\text{Ic}}/\sigma_{\text{uc}}$, the ratio between the mode I Griffith strength and the compression strength and is: $\alpha = 1 - c_1$; $K_{IIc}^2 = 1/c_{22}$; $K_{Ic}^2 = \alpha/c_{11} = (1 - c_1)/c_{11}$ and $3c_{122} = C\alpha c_{22}/K_{Ic} = 0.99\alpha/(K_{Ic} K_{IIc}^2) = 0.99c_{22}\sqrt{c_{11}(1 - c_1)}$.

If the ultimate compression stress is limited to be equal to the Griffith strength, then $\alpha = 1$ and $c_1 = 0$ and the relation between K_{Ic} and K_{IIc} is

$$K_{IIc}^2/K_{Ic}^2 = c_{11}/c_{22}. \quad (\text{A.9})$$

For higher compression stresses, the effective stress should be regarded [1], accounting for friction. This is not applied in practice.

Eq. (A.8) also follows from the exact derivation in [1] of this mixed mode strength based on the Airy stress function and it now is thus shown that the critical energy criterion is equal to the ultimate strength criterion.

According to [1], the ratio between K_{Ic} and K_{IIc} for plane stress is

$$K_{IIc}/K_{Ic} = 2\eta = 2(2 + \nu_{21} + \nu_{12})G_{xy}/E_y, \quad (\text{A.10})$$

where G_{xy} is the modulus of rigidity; E_y the modulus of elasticity and ν a contraction coefficient.

References

- [1] T.A.C.M. van der Put, A new fracture mechanics theory of orthotropic materials like wood, *Eng. Fract. Mech.* 74 (5) (2007) 771–781.
- [2] L. Nobile, C. Carloni, M. Nobile, Strain energy density prediction of crack initiation and direction in cracked T-beams and pipes, *Theor. Appl. Fract. Mech.* 41 (2004) 137–145.
- [3] G.C. Sih, P.C. Paris, G.R. Irwin, On cracks in rectilinearly anisotropic bodies, *Int. J. Fract. Mech.* 1 (1965) 189–203.
- [4] L. Bostrom, Method for determination of the softening behaviour of wood etc. Thesis, Report TVBM-1012, Lund, Sweden, 1992.
- [5] G.C. Sih, E. Baisch, Angled crack growth estimate with overshoot and/or overload, *Theor. Appl. Fract. Mech.* 18 (1992) 31–45.
- [6] I. Smith, E. Landis, Meng Gong, *Fracture and Fatigue in Wood*, Wiley, 2003.
- [7] T.A.C.M. van der Put, *Deformation and damage processes in wood*, Delft University Press, The Netherlands, 1989.
- [8] Y.W. May, On the velocity-dependent fracture toughness of wood, *Wood Science*, July 1975.
- [9] G.H. Valentin, L. Bostrom, P.J. Gustafsson, A. Ranta-Maunus, S. Gowda, RILEM state-of-the-art report on fracture mechanics, VTT Report 1262, Espoo, Finland, July 1991.
- [10] T.A.C.M. van der Put, Tensor polynomial failure criterion for wood polymers, Delft Wood Science Foundation Series 2 (2005). <www.dwsf.nl/downloads.htm>.